

Saturated-Unsaturated Flow in a Compressible Leaky-Unconfined Aquifer

Phoolendra K. Mishra^a, Velimir V. Vesselinov^a, Kristopher L. Kuhlman^b

^a*Computational Earth Sciences Group, Los Alamos National Laboratory, MS T003, Los Alamos, NM 87545, USA*

^b*Repository Performance Department, Sandia National Laboratories, 4100 National Parks Highway, Carlsbad, NM 88220, USA*

Abstract

An analytical solution is developed for three-dimensional flow towards a partially penetrating large-diameter well in an unconfined aquifer bounded below by a leaky aquitard of finite or semi-infinite extent. The analytical solution is derived using Laplace and Hankel transforms, then inverted numerically. Existing solutions for flow in leaky unconfined aquifers neglect the unsaturated zone following an assumption of instantaneous drainage due to Neuman. We extend the theory of leakage in unconfined aquifers by (1) including water flow and storage in the unsaturated zone above the water table, and (2) allowing the finite-diameter pumping well to partially penetrate the aquifer. The investigation of model-predicted results shows that aquitard leakage leads to significant departure from the unconfined solution without leakage. The investigation of dimensionless time-drawdown relationships shows that the aquitard drawdown also depends on unsaturated zone properties and the pumping-well wellbore storage effects.

Keywords: Unconfined aquifer, Aquitard, Leakage, Wellbore storage, unsaturated zone, Laplace-Hankel transform, Delayed piezometer response

1. Introduction

The assumption that the water flow and storage in the unsaturated zone is insignificant for unconfined aquifer tests was first questioned by Nwankwor et al. [1] and later by Akindunni and Gillham [2] based upon analysis of data collected during pumping tests in Borden,

5 Ontario Canada. Analyzing the collected tensiometer data and soil moisture measurements,
6 the authors concluded that the proper inclusion of unsaturated zone in analytical models
7 used for pumping test analysis would lead to improved estimates of aquifer specific yield.
8 Several analytical solutions were developed that account for the unsaturated zone flow to a
9 pumping well in an unconfined aquifer, taking into account the unsaturated zone [3, 4, 5].
10 These models consider the unsaturated zone effects by coupling the governing flow equations
11 at the water table; the saturated zone governed by the diffusion equation and the vadose
12 zone governed by the linearized unsaturated zone Richards equation, using the linearization
13 of Kroszynski and Dagan [6]. These models considered the limiting case where the pumping
14 well has zero radius. For detailed discussion regarding the fundamental differences between
15 these three models readers are directed to Mishra and Neuman [5].

16 Drawdown due to pumping a large-diameter (e.g., water supply) well in an unconfined
17 aquifer is affected by wellbore storage [7]. Narasimhan and Zhu [8] used a numerical model
18 to demonstrate that early time drawdown in an unconfined aquifer tends to be dominated
19 by wellbore storage effects. Mishra and Neuman [9] developed an analytical unconfined so-
20 lution, which considers both pumping-well wellbore storage capacity, and three-dimensional
21 axi-symmetrical unsaturated zone flow. They represented unsaturated zone constitutive
22 properties using exponential models, which result in governing equations that are mathe-
23 matically tractable, while being sufficiently flexible to be fit to other widely used constitutive
24 models [10, 11, 12, 13]. However, Mishra and Neuman [9] considered the unconfined aquifer
25 to be resting on an impermeable boundary and therefore did not account for the potential
26 effects of leakage from an underlying formation (e.g., an aquitard or fractured bedrock).
27 The classical theory of leakage for confined aquifers was originally developed by Hantush
28 [14] assuming steady-state vertical flow in overlying and underlying aquitards and horizon-
29 tal flow in the pumped aquifer. Hantush [15] later modified the theory of confined leaky
30 aquifers to include transient vertical aquitard flow, giving asymptotic expressions for early
31 and late times. Neuman and Witherspoon [16, 17] developed a more complete analytical
32 solution for the more general multiple aquifer flow problem, but did not consider general

33 three-dimensional aquitard flow.

34 Yatov [18] first investigated the effect of leakage from underlying strata on unconfined
35 aquifer flow. He use the model of Boulton [19] to account for the water table and considered
36 only vertical flow in aquitard. Ehlig and Halepaska [20] investigated leaky-unconfined flow
37 through a finite-difference simulation, which coupled the Boulton [19] and Hantush [14]
38 models to account for leakage across the aquifer-aquitard boundary. Zlotnik and Zhan [21]
39 developed an analytical solution for the flow towards a fully penetrating zero-radius well
40 in a coupled unconfined aquiferaquitard system where both the unsaturated zone and the
41 horizontal aquitard flow are neglected. Both Zhan and Bian [22] and Zlotnik and Zhan [21]
42 developed analytical and semi-analytical solutions for leakage due to pumping, building on
43 the works of Hantush [14] and Butler Jr and Tsou [23]. Both Zhan and Bian [22] and Zlotnik
44 and Zhan [21] neglect horizontal flow in aquitards. Purely vertical aquitard flow was justified
45 for limiting aquifer/aquitard hydraulic conductivity contrasts by Neuman and Witherspoon
46 [17]. Both Zhan and Bian [22] and Zlotnik and Zhan [21] only consider a vertically unbounded
47 aquitard. Malama et al. [24] developed a solution for three-dimensional aquitard flow in a
48 finite thickness aquitard, but considered the zero-radius pumping well to be fully penetrating
49 and ignored the flow in unsaturated zone. Here, we develop a more general leaky-unconfined
50 aquifer solution by considering a partially penetrating large-diameter well and including the
51 effects of unsaturated zone flow following Mishra and Neuman [9]. The solution is used
52 to investigate the effect of an aquitard on drawdown in overlying unconfined aquifer. We
53 conclude by investigating the effects of wellbore storage capacity and the unsaturated zone
54 on drawdown observed in the aquitard.

55 **2. Leaky-Unconfined Theory**

56 *2.1. Statement of Problem*

57 We consider an infinite radial compressible unconfined aquifer above a finitely thick
58 aquitard (Figure 1). The aquifer and aquitard are each spatially uniform, homogeneous and
59 anisotropic, with constant specific storage S_s and S_{s1} , respectively (a subscript 1 indicates

60 aquitard related properties). The aquifer has a fixed ratio $K_D = K_z/K_r$ between vertical and
61 horizontal saturated hydraulic conductivities, K_z and K_r , respectively. The aquitard vertical
62 and horizontal hydraulic conductivities are K_{z1} and K_{r1} . The aquifer is fully saturated
63 below an initially horizontal water table at elevation $z = b$. The water table is defined as a
64 $\psi = 0$ isobar where ψ is pressure head. A saturated capillary fringe at non-positive pressure
65 $\psi_a \leq \psi \leq 0$ extends from the water table to the $\psi = \psi_a$ isobar; $\psi_a \leq 0$ is the pressure
66 head required for air to enter a saturated medium. The saturated hydraulic system (aquifer
67 and aquitard) is at uniform initial hydraulic head $h_0 = b + \psi_a$ before pumping. At time
68 $t = 0$, pumping begins at a constant volumetric flowrate Q from a well of finite radius r_w
69 and wellbore storage coefficient C_w (volume of water released from storage in the pumping
70 well per unit drawdown in the well casing). The pumping well is completed across the
71 aquifer between depths l and d below the aquifer top. Under these conditions the drawdown
72 $s(r, z, t) = h(r, z, 0) - h(r, z, t)$ in the saturated zone is governed by the diffusion equation

$$K_r \frac{1}{r} \frac{\partial}{\partial r} \left(r \frac{\partial s}{\partial r} \right) + K_z \frac{\partial^2 s}{\partial z^2} = S_s \frac{\partial s}{\partial t} \quad r \geq r_w \quad 0 \leq z < b, \quad (1)$$

73 along with far-field boundary condition

$$s(\infty, z, t) = 0, \quad (2)$$

74 the no-flow condition at the portion of the well casing that is not open to the aquifer

$$\left(r \frac{\partial s}{\partial r} \right)_{r=r_w} = 0 \quad 0 \leq z \leq b-l \quad b-d \leq z \leq b, \quad (3)$$

75 and the wellbore storage mass-balance expression

$$2\pi K_r (l-d) \left(r \frac{\partial s}{\partial r} \right)_{r=r_w} - C_w \left(\frac{\partial s}{\partial t} \right)_{r=r_w} = -Q \quad b-l \leq z \leq b-d. \quad (4)$$

76 Flux is assumed constant across the well screen (see Zhan and Zlotnik [25] for a discussion
77 of this assumption's validity). The corresponding linearized unsaturated flow equations [5]
78 are

$$K_r k_0(z) \frac{1}{r} \frac{\partial}{\partial r} \left(r \frac{\partial \sigma}{\partial r} \right) + K_z \frac{\partial}{\partial z} \left(k_0(z) \frac{\partial \sigma}{\partial z} \right) = C_0(z) \frac{\partial \sigma}{\partial t} \quad (5)$$

$$r \geq r_w \quad b < z < b+L$$

79 where $\sigma(r, z, t)$ is drawdown in the unsaturated zone, $k_0(z)$ is relative permeability and
 80 $C_0(z)$ is moisture capacity (slope of the curve representing water saturation as a function
 81 of pressure head) functions with the functional dependence limitations on the respective
 82 constitutive models

$$k_0(z) = k(\theta_0), \quad C_0(z) = C(\theta_0) \quad (6)$$

83 where θ_0 is the initial volumetric moisture content. Equation (5) depends on the initial
 84 condition

$$\sigma(r, z, 0) = 0, \quad (7)$$

85 the far-field boundary condition

$$\sigma(\infty, z, t) = 0 \quad (8)$$

86 the no-flow condition at the ground surface

$$\left. \frac{\partial \sigma}{\partial z} \right|_{z=b+L} = 0 \quad r \geq r_w \quad (9)$$

87 and the no-flow condition at the well casing

$$\left(r \frac{\partial \sigma}{\partial r} \right)_{r=r_w} = 0 \quad b < z < b + L. \quad (10)$$

88 The interface conditions providing continuity across the water table are

$$s - \sigma = 0 \quad r \geq r_w \quad z = b, \quad (11)$$

$$\frac{\partial s}{\partial z} - \frac{\partial \sigma}{\partial z} = 0 \quad r \geq r_w \quad z = b. \quad (12)$$

89 The aquitard drawdown $s_1(r, z, t)$ is governed by

$$K_{r1} \frac{1}{r} \frac{\partial}{\partial r} \left(r \frac{\partial s_1}{\partial r} \right) + K_{z1} \frac{\partial^2 s_1}{\partial z^2} = S_{s1} \frac{\partial s_1}{\partial t} \quad r \geq 0 \quad -b_1 \leq z < 0. \quad (13)$$

90 Additionally, aquitard flow satisfies no-flow conditions at the bottom and center of the flow
 91 system

$$\lim_{r \rightarrow 0} \left(r \frac{\partial s_1}{\partial r} \right) = \left. \frac{\partial s_1}{\partial z} \right|_{z=-b_1} = 0. \quad (14)$$

92 The interface condition across the aquifer-aquitard boundary are

$$s - s_1 = 0 \quad r \geq r_w \quad z = 0 \quad (15)$$

93 and

$$K_z \frac{\partial s}{\partial z} = K_{z1} \frac{\partial s_1}{\partial z} \quad r \geq r_w \quad z = 0. \quad (16)$$

94 Like Mishra and Neuman [5], we represent the aquifer moisture retention curve using an
 95 exponential function

$$S_e = \frac{\theta(\psi) - \theta_r}{S_y} = e^{a_c(\psi - \psi_a)} \quad a_c \geq 0 \quad \psi_a \geq 0 \quad (17)$$

96 where θ_r is residual volumetric water content, $S_y = \theta_s - \theta_r$ is drainable porosity or spe-
 97 cific yield and S_e is effective saturation. We also adopt the exponential relative hydraulic
 98 conductivity model [10],

$$k(\psi) = \begin{cases} e^{a_k(\psi - \psi_k)} & \psi \leq \psi_k \\ 1 & \psi > \psi_k \end{cases} \quad a_k \geq 0 \quad \psi_k \geq 0, \quad (18)$$

99 with parameters a_k and ψ_k that generally differ from a_c and ψ_a in (17). The parameters
 100 a_k and a_c represent the exponent in the exponential models for hydraulic conductivity and
 101 effective saturation, respectively. The parameter ψ_k represents a pressure head above which
 102 relative hydraulic conductivity is effectively equal to unity, which is sometimes but not always
 103 equal to the air entry pressure head ψ_a . In addition to rendering the resulting equations
 104 mathematically tractable, these exponential constitutive models are sufficiently flexible to
 105 provide acceptable fits to standard constitutive models such as those mentioned earlier.

106 2.2. Point drawdown in saturated and unsaturated zones of aquifer and aquitard

107 Following Mishra and Neuman [9], it is shown in Appendix A that, drawdown in the
 108 saturated zone can be expressed as

$$s = s_C + s_U \quad (19)$$

109 where s_C is solution for flow to a partially penetrating well of finite radius in a confined aquifer
 110 and s_U is a correction accounting for the underlying aquitard, water table and unsaturated
 111 zone effects. The Laplace transformed solution \bar{s}_C is given by Mishra and Neuman [9] as

$$\bar{s}_C(r_D, z_D, p_D) = \frac{Q}{4\pi T p_D} \omega_0 K_0(\phi_0) + \sum_{n=1}^{\infty} \omega_n K_0(\phi_n) \cos[n\pi(1 - z_d)] \quad (20)$$

$$r_d \geq r_w/b$$

112 where $\omega_n = \frac{\sin(n\pi l_D) - \sin(n\pi d_D)}{n\pi(l_D - d_D)\Omega(n)}$, $\Omega(n) = r_{wD}\phi_0 K_1(r_{wD}\phi_n) + \frac{C_{wD}}{2(l_D - d_D)} r_{wD}^2 \phi_n^2 K_0(r_{wD}\phi_n)$, $\omega_0 =$
 113 $2/\Omega(0)$, $r_{wD} = r_w/r$, $r_D = r/b$, $z_D = z/b$, $d_D = d/b$, $l_D = l/b$, $p_D = pt$, $C_{wD} = C_w/(\pi S_s b r_w^2)$,
 114 $t_s = \alpha_s t/r^2$, p is Laplace parameter (the transform of t), $\phi_n = \sqrt{p_D/t_s + r_D^2 K_D n^2 \pi^2}$, and K_0
 115 and K_1 are second-kind modified Bessel functions of orders zero and one. The Laplace trans-
 116 formed unsaturated zone drawdown $\bar{\sigma}$ is given by Mishra and Neuman [9] and is presented
 117 in Appendix D for sake of completeness.

118 The Laplace transformed \bar{s}_U derived in Appendix B is

$$\bar{s}_U(r_D, z_D, p_D) = \int_0^{\infty} (\rho_1 e^{\mu z_D} + \rho_2 e^{-\mu z_D}) \frac{r_D^2 K_D}{r^2} y J_0 \left[y K_D^{1/2} r_D \right] dy \quad (21)$$

119 where $\rho_1 = \frac{(\frac{\mu}{q_b} + 1)e^{-\mu(\bar{s}_c)_{z_D=0}} - (\frac{\mu}{q_1 b} + 1)e^{-\mu(\bar{s}_c)_{z_D=1}}}{\Delta}$, $\rho_2 = \frac{(\frac{\mu}{q_b} - 1)e^{-\mu(\bar{s}_c)_{z_D=0}} - (\frac{\mu}{q_1 b} - 1)e^{-\mu(\bar{s}_c)_{z_D=1}}}{\Delta}$, $q_1 b =$
 120 $R_{K_z} \mu_1 \tanh(\mu_1 R_b)$, $\mu_1^2 = \frac{y^2}{R_{K_D}} + \frac{p_D}{t_s K_D r_D^2 R_{K_D} R_{\alpha_s}}$, $R_{K_D} = K_{D1}/K_D$, $R_{K_z} = K_{z1}/K_z$, $R_{\alpha_s} =$
 121 α_{S1}/α_s , $R_b = b_1/b$, $\alpha_{s1} = K_{r1}/S_{s1}$, and $\Delta = \left(\frac{\mu}{q_b} + 1\right) \left(\frac{\mu}{q_1 b} - 1\right) e^{-\mu} - \left(\frac{\mu}{q_b} - 1\right) \left(\frac{\mu}{q_1 b} + 1\right) e^{\mu}$.

122 The Laplace transformed aquitard drawdown derived in Appendix C is

$$\bar{s}_1(r_D, z_D, p_D) = \int_0^{\infty} \frac{(\bar{s}_c)_{z_D=0} + \rho_1 + \rho_2}{\cosh(\mu_1 b_1/b)} \cosh[\mu_1(z_D + R_b)] \quad (22)$$

$$\times \frac{r_D^2 K_D}{r^2} y J_0 \left[y K_D^{1/2} r_D \right] dy$$

123 where $(\bar{s}_c)_{z_D=0}$ is the Laplace-Hankel transformed confined aquifer drawdown and is defined
 124 in Appendix D. The time domain equivalents s_C , s_U , s_1 and σ of \bar{s}_C , \bar{s}_U , \bar{s}_1 and $\bar{\sigma}$ are
 125 obtained through numerical Laplace transform inversion using the algorithm of de Hoog
 126 et al. [26].

127 *2.3. Vertically Averaged Drawdown in Piezometer or Observation Well*

128 Drawdown in an observation well (Figure 1) that is completed in the aquifer between
 129 elevations $z_{D1} = z_1/b$ and $z_{D2} = z_2/b$ is found by averaging the point drawdown over screen
 130 interval,

$$s_{z_{D2}-z_{D1}}(r_D, t_s) = \frac{1}{z_{D2} - z_{D1}} \int_{z_{D1}}^{z_{D2}} s^*(r_D, z_D, t_s) dz_D \quad (23)$$

131 where s^* can be either aquifer drawdown s , aquitard drawdown s_1 , or a combination of the
 132 two, depending on the observation well screen interval.

133 *2.4. Delayed Piezometer or Observation Well Response*

134 When water level is measured in a piezometer or observation well having storage coeffi-
 135 cient C the water level observed in the borehole is delayed in time. Following Mishra and
 136 Neuman [9], the measured (delayed) drawdown s_m can be expressed in terms of formation
 137 drawdown s via

$$s_m = s (1 - e^{-t/t_B}) \quad (24)$$

138 where t_B is basic (characteristic) monitoring well time lag. The dimensionless equivalent of
 139 (24) is

$$s_{mD} = s_D (1 - e^{-t_s/t_{Bs}}) \quad (25)$$

140 where $t_{Bs} = \alpha_s t_B / r^2$, and r is the radial distance to the monitoring location.

141 **3. Model-predicted drawdown behavior**

142 We illustrate the impacts of an underlying aquitard on unconfined aquifer drawdown for
 143 the case where $K_D = 1$, $S_s b / S_y = 10^{-3}$, $a_{kD} = a_{cD} = 10$, $\psi_{aD} = \psi_{kD}$, $d_D = 0$, $C_{wD} = 10^3$,
 144 $l_D = 0.6$ and $r_w/b = 0.02$, where $a_{kD} = a_k b$, $a_{cD} = a_c b$, $\psi_{aD} = \psi_a/b$ and $\psi_{kD} = \psi_k/b$. We also
 145 investigate the effects that wellbore storage capacity of the pumping well, the unconfined
 146 aquifer, and the unsaturated zone have on aquitard drawdown.

147 *3.1. Dimensionless unconfined aquifer time-drawdown*

148 We start by considering drawdown at two locations in the unconfined aquifer saturated
 149 zone, one location closer to water table ($z_D = 0.75$) and the other closer to the aquitard-
 150 aquifer boundary ($z_D = 0.25$). Figures 2a and 2b compare variations in dimensionless
 151 drawdown $s_D(r_D, z_d, t_s) = (4\pi K_r b/Q)s(r_D, z_D, t_s)$ with dimensionless time at $z_D = 0.75$ and
 152 $z_D = 0.25$ predicted by our proposed solution and the solutions of Mishra and Neuman
 153 [9], Neuman [27], and the modified solution of Malama et al. [24] (modified to include the
 154 partially penetrating pumping well effects, as done in Malama et al. [28] for a multi-aquifer
 155 system). The solutions of Neuman [27] and Malama et al. [24] do not include wellbore storage
 156 effects, and therefore they overestimate drawdown at early time. Both of these solutions also
 157 ignore the unsaturated zone above the water table, considering the water table a material
 158 boundary [27]. Our proposed solution follows Mishra and Neuman [9] when leakage effects
 159 are minor, but our solution predicts less drawdown when leakage effects are significant. It
 160 is seen in Figure 2b that solution of Mishra and Neuman [9] overestimates drawdown near
 161 the aquitard at intermediate time because it does not include aquitard leakage. Near the
 162 water table (Figure 2a) the effects of aquitard leakage are minimal and our proposed solution
 163 approaches Mishra and Neuman [9] at all times.

164 Figures 3a and 3b show dimensionless time-drawdown variations at dimensionless radial
 165 distance $r_D = 0.5$ and dimensionless unconfined aquifer saturated zone elevation $z_D = 0.25$
 166 with different values of $R_{K_z} = K_{z1}/K_z$ when the radial aquitard hydraulic conductivity is
 167 small ($R_{K_r} = K_{r1}/K_r = 10^{-6}$) and large ($R_{k_r} = 1.0$). When the radial hydraulic conductivity
 168 in aquitard is negligible ($R_{k_r} = 10^{-6}$), aquitard flow is predominately vertical; larger values
 169 of vertical aquitard hydraulic conductivity cause decreases in intermediate time drawdown
 170 (Figure 3a). It is seen from Figure 3b that when aquitard horizontal hydraulic conductivity is
 171 large ($R_{k_r} = 1$) the amount drawdown is reduced from further increases in aquitard vertical
 172 hydraulic conductivity also extend to the later time.

173 Figure 4 depicts the effect of R_{K_r} on the dimensionless time-drawdown at dimensionless
 174 radial distance $r_D = 0.5$ and dimensionless unconfined aquifer saturated zone elevation

175 $z_D = 0.25$ when $R_{K_z} = 0.1$. Radial flow in the aquitard results in less drawdown at late time
176 than that predicted by Mishra and Neuman [9], who do not account for aquitard leakage.

177 Figure 5 presents the effect of hydraulic conductivity of an isotropic aquitard on di-
178 mensionless time-drawdown at dimensionless radial distance $r_D = 0.5$ and dimensionless
179 unconfined aquifer saturated zone elevation $z_D = 0.25$. When aquitard hydraulic conduc-
180 tivity is at least two orders of magnitude smaller than the unconfined aquifer, the effects
181 of leakage on the aquifer drawdown are negligible. This is in agreement with findings of
182 Neuman and Witherspoon [16] for confined aquifers. They found errors $< 5\%$ attributable
183 to the vertical aquitard flow assumption, when the hydraulic conductivity contrast between
184 the aquifer and aquitard was greater than a factor of 100. Figure 5 also presents a case
185 with the aquitard hydraulic conductivity is larger than the aquifer. Because the proposed
186 model accounts for general three-dimensional flow in underlying zone, we can consider the
187 case where the lower layer is more permeable than the aquifer ($R_{k_r} = 2$).

188 Figure 6 shows how the dimensionless unconfined aquifer time-drawdown is affected by
189 aquitard thickness. When the aquitard thickness is less than the initial unconfined aquifer
190 saturated thickness ($R_b \leq 1$) aquitard leakage only affects the time-drawdown curve at
191 intermediate time. Figure 6 shows that further increases in aquitard thickness beyond eight
192 times the initial unconfined aquifer saturated zone thickness have negligible effect on the
193 time-drawdown curve.

194 3.2. Dimensionless aquitard time-drawdown

195 Figure 7 depicts dimensionless aquitard drawdown $s_D(r_D, z_d, t_s) = (4\pi K_r b/Q) s_1(r_D, z_D, t_s)$
196 variations with dimensionless time at dimensionless radial distance $r_D = 0.2$ and dimension-
197 less aquitard elevation $z_D = -0.25$ for different values of C_{wD} . As with solution of Mishra
198 and Neuman [9] for non-leaky systems, aquitard drawdown is impacted by pumping-well
199 wellbore storage capacity. Larger wellbore storage factors result in increased capacity of the
200 wellbore to store water, resulting in a delay in the aquitard time-drawdown, as indicated in
201 Figure 7.

202 Figure 8 depicts the effect that changes in a_{kD} , the dimensionless relative hydraulic con-

203 ductivity exponent, have on dimensionless time-drawdown at dimensionless radial distance
 204 $r_D = 0.2$ and dimensionless aquitard elevation $z_D = -0.25$. For larger values of s_{kD} , the
 205 unsaturated zone hydraulic conductivity decreases more rapidly as pressure becomes more
 206 negative, relative to the threshold pressure ψ_k . A diminishing rate of water then drains from
 207 the vadose zone into the aquifer; this drainage contributes to reduced aquitard drawdown.
 208 For very large a_{kD} , unsaturated hydraulic conductivity quickly decreases once pressure head
 209 is below ψ_k , which leads to a much less permeable unsaturated zone.

210 Figure 9 shows the effects that changes in a_{cD} , the dimensionless effective saturation
 211 exponent, have on dimensionless time-drawdown at dimensionless radial distance $r_D = 0.2$
 212 and dimensionless aquitard elevation $z_D = -0.25$. When a_{cD} and a_{kD} are both large,
 213 pressure head and hydraulic conductivity in the vadose zone quickly reduce as pressure
 214 reaches the thresholds ψ_k and ψ_a . The vadose zone can no longer store water, and the water
 215 table essentially becomes a moving boundary, which leads to the limiting-case behavior of
 216 instantaneous drainage due to Neuman [27]. Consequently, for large values of exponents
 217 (Figure 9, red curve) the proposed solution reduces to that of Malama et al. [24], which
 218 relies on the assumption of instantaneous drainage of Neuman [27]. As a_{cD} decreases, the
 219 vadose zone has increased capacity to store water, which diminishes the water table response
 220 and aquifer drawdown increases, compared to that predicted by Malama et al. [24].

221 4. Conclusions

222 Our work leads to the following major conclusions:

- 223 1. A new analytical solution was developed for axially symmetric saturated-unsaturated
 224 three dimensional radial flow to a well with wellbore storage that partially penetrates
 225 the saturated zone of a compressible vertically anisotropic leaky-unconfined aquifer.
 226 The solution accounts for both radial and vertical flow in the unsaturated zone and
 227 the underlying aquitard.
- 228 2. Because the solution considers three-dimensional radial flow in the aquitard, any prop-
 229 erties may be assigned to the aquitard, allowing the solution to also be used to simulate

- 230 leakage from underlying non-aquitard layers (e.g., an unscreened aquifer region with
231 different hydraulic properties).
- 232 3. Aquitard leakage can lead to significant departures from solutions that do not account
233 for leakage, e.g., Mishra and Neuman [9]. However, the effect of leakage on uncon-
234 fined aquifer drawdown diminishes at points farther away from the aquifer-aquitard
235 boundary.
 - 236 4. Unsaturated zone effects are often more important than leakage effects when the ob-
237 servation location is close to the water table.
 - 238 5. For large diameter pumping wells, at early time water is withdrawn entirely from the
239 wellbore storage. Solution that do not account for wellbore storage predict a much
240 larger early rise in drawdown.
 - 241 6. Aquitard drawdown is also affected by the pumping-well wellbore storage capacity. As
242 in the unconfined aquifer, larger wellbore storage capacity leads to larger impacts on
243 the observed aquitard drawdown.
 - 244 7. The unsaturated zone properties not only affect the unconfined aquifer time-drawdown
245 behavior but they also impact the observed aquitard response.

246 **Acknowledgments**

247 This research was partially funded by the Environmental Programs Directorate of the
248 Los Alamos National Laboratory. Los Alamos National Laboratory is a multi-program lab-
249 oratory managed and operated by Los Alamos National Security (LANS) Inc. for the U.S.
250 Department of Energys National Nuclear Security Administration under contract DE-AC52-
251 06NA25396. Sandia National Laboratories is a multi-program laboratory managed and oper-
252 ated by Sandia Corporation, a wholly owned subsidiary of Lockheed Martin Corporation, for
253 the U.S. Department of Energys National Nuclear Security Administration under contract
254 DE-AC04-94AL85000.

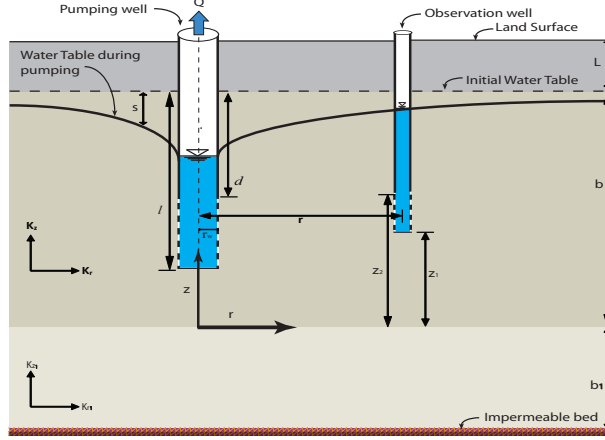


Figure 1: Schematic representation of leaky unconfined aquifer-aquitard system geometry with finite radius pumping well

255 Appendix A. Decomposition of saturated zone solution

256 In a manner analogous to Mishra and Neuman [5] we decompose s into two parts

$$s = s_C + s_U \quad (\text{A.1})$$

257 where s_C is solution for a partially penetrating well in a confined aquifer, satisfying

$$\frac{1}{r} \frac{\partial}{\partial r} \left(r \frac{\partial s_C}{\partial r} \right) + K_D \frac{\partial^2 s_C}{\partial z^2} = \frac{1}{\alpha_s} \frac{\partial s_C}{\partial t} \quad r \geq r_w \quad 0 \leq z < b \quad (\text{A.2})$$

258

$$s_C(r, z, 0) = 0 \quad r \geq r_w \quad (\text{A.3})$$

259

$$s_C(\infty, z, t) = 0 \quad (\text{A.4})$$

260

$$\left. \frac{\partial s_C}{\partial z} \right|_{z=(0,b)} = 0 \quad r \geq r_w \quad (\text{A.5})$$

261

$$\left(\frac{\partial s_C}{\partial r} \right)_{r=r_w} = 0 \quad 0 \leq z \leq b-l \quad b-d \leq z \leq b \quad (\text{A.6})$$

Table 1: **Fundamental Properties Table**

a	Hankel transform parameter	L^{-1}
a_c	exponent in moisture retention curve or sorptive number	L^{-1}
a_k	exponent in Gardner relative hydraulic conductivity model	L^{-1}
b	saturated thickness of unconfined aquifer before pumping begins	L
b_1	thickness of aquitard	L
C_w	wellbore storage coefficient	L^2
d	distance from top of screened interval to top of aquifer	L
h	hydraulic head (sum of pressure and elevation heads)	L
K_r	aquifer radial hydraulic conductivity	LT^{-1}
K_{r1}	aquitard radial hydraulic conductivity	LT^{-1}
K_z	aquifer vertical hydraulic conductivity	LT^{-1}
K_{z1}	aquitard vertical hydraulic conductivity	LT^{-1}
l	distance from bottom of screened interval to top of aquifer	L
L	thickness of vadose zone before pumping begins	L
n	finite cosine transform parameter	–
p	Laplace transform parameter	T^{-1}
Q	volumetric pumping rate	L^3T^{-1}
r	radial distance from the center of pumping well	L
r_w	diameter of pumping well	L
s	drawdown in aquifer; change in hydraulic head since pumping began	L
s_1	drawdown in aquitard; change in hydraulic head since pumping began	L
S_e	effective saturation	–
S_s	aquifer specific storage	L^{-1}
S_{s1}	aquitard specific storage	L^{-1}
S_y	aquifer drainable porosity or specific yield	–
t	time since pumping began	T
z	vertical distance from the bottom of the aquifer, positive up	L
z_i	elevation to top ($i = 1$) and bottom ($i = 2$) of monitoring interval	L
θ_0	initial volumetric water content	–
θ_r	residual volumetric water content	–
θ_s	saturated volumetric water content	–
σ	drawdown in unsaturated zone; change in hydraulic head since pumping began	L
ψ	pressure head (less than zero when unsaturated)	L
ψ_a	air-entry pressure	L
ψ_k	pressure for saturated hydraulic conductivity ₁₄	L

Table 2: **Derived quantities table**

K_D	K_z/K_r	Anisotropy ratio
r_D	r/b	dimensionless radial coordinate
z_D	z/b	dimensionless vertical coordinate
d_D	d/b	dimensionless distance to top of screen interval
l_D	l/b	dimensionless distance to bottom of screen interval
p_D	pt	dimensionless Laplace parameter
r_{wD}	r_w/r	dimensionless well radius
R_{K_D}	K_{D1}/K_D	ratio of aquitard and aquifer anistropies
R_{K_r}	K_{r1}/K_r	ratio of aquitard and aquifer horizontal hydraulic conductivities
R_{K_z}	K_{z1}/K_z	ratio of aquitard and aquifer vertical hydraulic conductivities
R_{α_s}	α_{s1}/α_s	ratio of aquitard and aquifer saturated hydraulic diffusivities
R_b	b_1/b	ratio of aquitard and aquifer thicknesses
α_s	K_r/S_s	aquifer hydraulic diffusivity
α_{s1}	K_{r1}/S_{s1}	aquitard hydraulic diffusivity
z_{D_i}	z_i/b	dimensionless elevation to top ($i = 1$) and bottom ($i = 2$) of monitoring interval
a_{kD}	$a_k b$	dimensionless Gardner hydraulic conductivity model exponent
a_{cD}	$a_c b$	dimensionless moisture retention model exponent
ψ_{aD}	ψ_a/b	dimensionless air-entry pressure
ψ_{kD}	ψ_k/b	dimensionless pressure for saturated hydraulic conductivity
C_{wD}	$C_w/(\pi S_s b r_w^2)$	dimensionless wellbore storage coefficient
t_s	$\alpha_s t/r^2$	dimensionless time

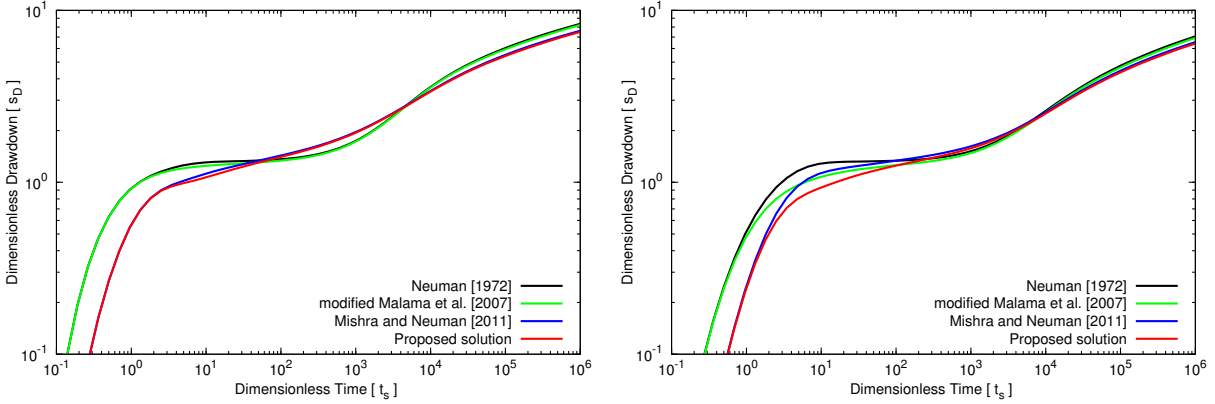


Figure 2: Dimensionless leaky-unconfined aquifer drawdown versus dimensionless time at $r_D = 0.5$ when $K_D = 1$, $S_S b/S_y = 10^{-3}$, $a_{kD} = a_{cD} = 10$, $\psi_{aD} = \psi_{kD}$, $d_D = 0$, $l_D = 0.6$, $C_{wD} = 10^2$, $R_{K_r} = R_{K_z} = 10^{-2}$, $R_{S_s} = 10^{-2}$, $R_b \rightarrow \infty$ and (a) $z_D = 0.75$ (b) $z_D = 0.25$. Solutions of Mishra and Neuman [9], modified Malama et al. [24], and Neuman [27] are also shown.

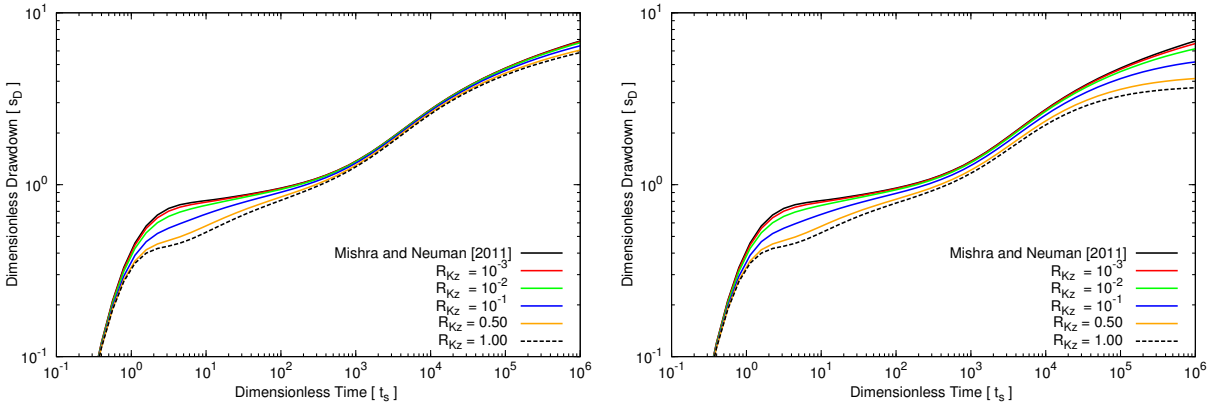


Figure 3: Dimensionless leaky-unconfined aquifer drawdown versus dimensionless time at $r_D = 0.5$ and $z_D = 0.25$ for $K_D = 1$, $S_S b/S_y = 10^{-3}$, $a_{kD} = a_{cD} = 10$, $\psi_{aD} = \psi_{kD}$, $d_D = 0$, $l_D = 0.6$, $C_{wD} = 10^2$, $R_{S_s} = 10^{-2}$, $R_b \rightarrow \infty$ when R_{K_z} varies and (a) $R_{K_r} = 10^{-6}$ (b) $R_{K_r} = 1$. Solution of Mishra and Neuman [9] is also shown.

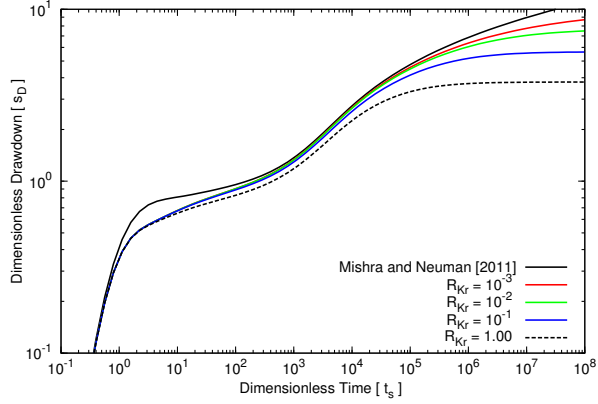


Figure 4: Dimensionless leaky-unconfined aquifer drawdown versus dimensionless time at $r_D = 0.5$ and $z_D = 0.25$ for $K_D = 1$, $S_S b/S_y = 10^{-3}$, $a_{kD} = a_{cD} = 10$, $\psi_{aD} = \psi_{kD}$, $d_D = 0$, $l_D = 0.6$, $C_{wD} = 10^2$, $R_{S_s} = 10^{-2}$, $R_{K_z} = 0.1$ and $R_b \rightarrow \infty$ when R_{K_r} varies. Solution of Mishra and Neuman [9] is also shown.

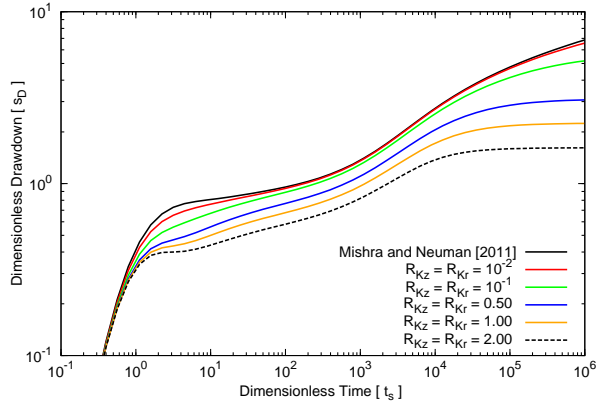


Figure 5: Dimensionless leaky-unconfined aquifer drawdown versus dimensionless time at $r_D = 0.5$ and $z_D = 0.25$ for $K_D = 1$, $S_S b/S_y = 10^{-3}$, $a_{kD} = a_{cD} = 10$, $\psi_{aD} = \psi_{kD}$, $d_D = 0$, $l_D = 0.6$, $C_{wD} = 10^2$, $R_b \rightarrow \infty$ when $R_{K_z} = R_{K_r}$ varies and $R_{S_s} = 1$. Solution of Mishra and Neuman [9] is also shown.

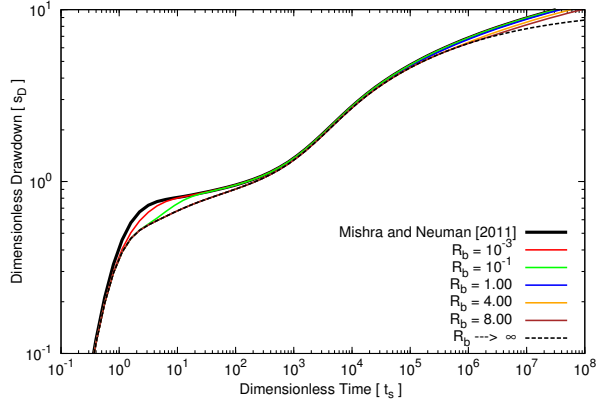


Figure 6: Dimensionless leaky-unconfined aquifer drawdown versus dimensionless time at $r_D = 0.5$ and $z_D = 0.25$ for $K_D = 1$, $S_S b/S_y = 10^{-3}$, $a_{kD} = a_{cD} = 10$, $\psi_{aD} = \psi_{kD}$, $d_D = 0$, $l_D = 0.6$, $C_{wD} = 10^2$, $R_{S_s} = 10^2$, $R_{K_z} = R_{K_r} = 10^{-2}$ when $R_b = b_1/b$ varies. Solution of Mishra and Neuman [9] is also shown.

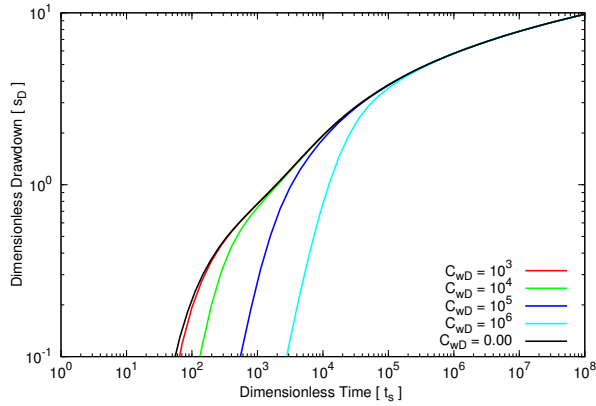


Figure 7: Dimensionless aquitard drawdown versus dimensionless time at $r_D = 0.2$ and $z_D = -0.25$ for $K_D = 1$, $S_S b/S_y = 10^{-3}$, $a_{kD} = a_{cD} = 10$, $\psi_{aD} = \psi_{kD}$, $d_D = 0$, $l_D = 0.6$, $R_{S_s} = 10^2$, $R_{K_z} = R_{K_r} = 10^{-2}$, $R_b \rightarrow \infty$ when C_{wD} , the dimensionless wellbore storage varies.

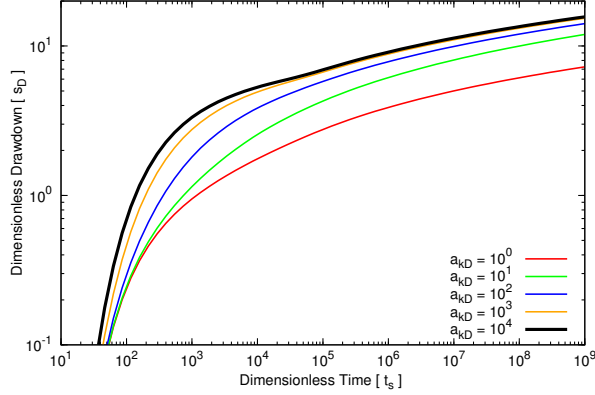


Figure 8: Dimensionless aquitard drawdown versus dimensionless time at $r_D = 0.2$ and $z_D = -0.25$ for $K_D = 1$, $S_{Sb}/S_y = 10^{-3}$, $\psi_{aD} = \psi_{kD}$, $d_D = 0$, $l_D = 0.6$, $C_{wD} = 10^2$, $R_{S_z} = 10^2$, $R_{K_z} = R_{K_r} = 10^{-2}$, $R_b \rightarrow \infty$ when, $a_{cD} = 1$ and a_{kD} varies.

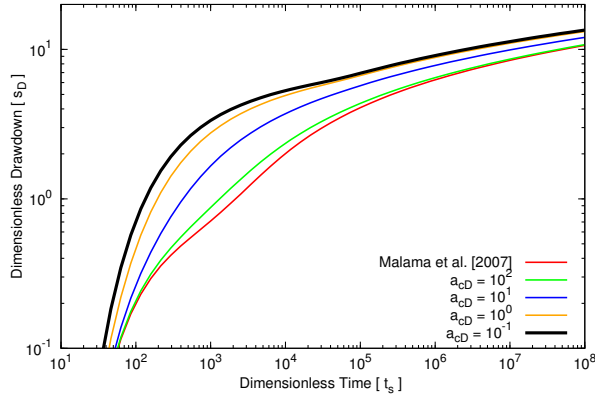


Figure 9: Dimensionless aquitard drawdown versus dimensionless time at $r_D = 0.2$ and $z_D = -0.25$ for $K_D = 1$, $S_{Sb}/S_y = 10^{-3}$, $\psi_{aD} = \psi_{kD}$, $d_D = 0$, $l_D = 0.6$, $C_{wD} = 10^2$, $R_{S_z} = 10^2$, $R_{K_z} = R_{K_r} = 10^{-2}$, $R_b \rightarrow \infty$ when, $a_{kD} = 10^3$ and a_{cD} varies.

$$2\pi K_r (l - d) \left. \frac{\partial s_C}{\partial r} \right|_{r=r_w} - C_W \left. \frac{\partial s_C}{\partial t} \right|_{r=r_w} = -Q \quad b - l \leq z \leq b - d \quad (\text{A.7})$$

263 and s_U is a solution that takes into account aquitard and saturated-unsaturated unconfined
264 conditions, but has no pumping source term, satisfying

$$\frac{1}{r} \frac{\partial}{\partial r} \left(r \frac{\partial s_U}{\partial r} \right) + K_D \frac{\partial^2 s_U}{\partial z^2} = \frac{1}{\alpha_s} \frac{\partial s_U}{\partial t} \quad (\text{A.8})$$

$$r \geq 0 \quad 0 \leq z < b$$

265

$$s_U(r, z, 0) = 0 \quad r \geq 0 \quad (\text{A.9})$$

266

$$s_U(\infty, z, t) = 0 \quad (\text{A.10})$$

267

$$\frac{\partial s_U}{\partial z} - \frac{K_{z1}}{K_z} \frac{\partial s_1}{\partial z} = 0 \quad r \geq 0 \quad z = 0 \quad (\text{A.11})$$

268

$$\left. \frac{\partial s_U}{\partial z} \right|_{r=0} = 0 \quad 0 \leq z \leq b \quad (\text{A.12})$$

269 subject to interface conditions at water table,

$$s_C + s_U - \sigma = 0 \quad r \geq r_w \quad z = b \quad (\text{A.13})$$

270

$$\frac{\partial s_C}{\partial z} + \frac{\partial s_U}{\partial z} - \frac{\partial \sigma}{\partial z} = 0 \quad r \geq r_w \quad z = b, \quad (\text{A.14})$$

271 where the first term is zero by definition of s_C .

272 **Appendix B. Laplace-space solution for saturated zone**

273 Equations (A.8)–(A.14) are solved by sequential application of the Hankel transform

$$f(a) = \int_0^{\infty} r J_0(ar) f(r) dr \quad (\text{B.1})$$

274 and Laplace transform

$$f(p) = \int_0^{\infty} f(t) e^{-pt} dt \quad (\text{B.2})$$

275 with Hankel parameter a and Laplace parameter p , J_0 being zero-order Bessel function of
276 the first kind.

277 The Laplace-Hankel transform of confined aquifer solution [9] is

$$\begin{aligned} \bar{\bar{s}}_C(a, z_D, p_D) &= C_0 \left\{ \frac{r_w}{a} J_1(ar_w) K_0(r_w \tau_0) \right. \\ &\quad \left. + \frac{\tau_0 r_w J_0(ar) K_1(r \tau_0) - ar_w J_1(ar) K_0(r \tau_0)}{a^2 + \tau_0^2} \right\} \\ &\quad + \sum_{n=1}^{\infty} C_n \left\{ \frac{r_w}{a} J_1(ar_w) K_0(r_w \tau_0) \right. \\ &\quad \left. + \frac{\tau_n r_w J_0(ar) K_1(r \tau_n) - ar_w J_1(ar) K_0(r \tau_n)}{a^2 + \tau_n^2} \right\} \\ &\quad \times \cos[n\pi(1 - z_D)] \end{aligned} \quad (\text{B.3})$$

278 where $\tau_0 = \sqrt{pS_s/K_r}$ and $\tau_n = \sqrt{pS_s/K_r + K_D n^2 \pi^2 / b^2}$.

279 The Laplace transform of (A.8)–(A.14) is

$$\frac{1}{r} \frac{\partial}{\partial r} \left(r \frac{\partial \bar{s}_U}{\partial r} \right) + K_D \frac{\partial^2 \bar{s}_U}{\partial z^2} = \frac{p}{\alpha_s} \bar{s}_U \quad 0 \leq z < b \quad (\text{B.4})$$

280

$$\bar{s}_U(\infty, z, p) = 0 \quad (\text{B.5})$$

281

$$\left. \frac{\partial \bar{s}_U}{\partial z} \right|_{z=0} = \frac{K_{z1}}{K_z} \frac{\partial \bar{s}_1}{\partial z} \quad (\text{B.6})$$

282

$$\left(r \frac{\partial \bar{s}_U}{\partial r} \right)_{r=0} = 0 \quad 0 \leq z \leq b \quad (\text{B.7})$$

283

$$\bar{s}_C + \bar{s}_U - \bar{\sigma} = 0 \quad z = b \quad (\text{B.8})$$

284

$$\frac{\partial \bar{s}_C}{\partial z} + \frac{\partial \bar{s}_U}{\partial z} - \frac{\partial \bar{\sigma}}{\partial z} = 0 \quad z = b \quad (\text{B.9})$$

285 where the first term is zero by definition of \bar{s}_C .

286 Taking the Hankel transform of (B.4)–(B.9) yields

$$-a^2 \bar{s}_U + K_D \frac{\partial^2 \bar{s}_U}{\partial z^2} = \frac{p}{\alpha_s} \bar{s}_U \quad 0 \leq z < b \quad (\text{B.10})$$

287

$$\bar{s}_H + \bar{s}_U - \bar{\sigma} = 0 \quad z = b \quad (\text{B.11})$$

288

$$\frac{\partial \bar{s}_H}{\partial z} + \frac{\partial \bar{s}_U}{\partial z} - \frac{\partial \bar{\sigma}}{\partial z} = 0 \quad z = b \quad (\text{B.12})$$

289

$$\frac{\partial \bar{s}_C}{\partial z} + \frac{\partial \bar{s}_U}{\partial z} - \frac{K_{z1}}{K_z} \frac{\partial \bar{s}_1}{\partial z} = 0 \quad z = 0 \quad (\text{B.13})$$

290 The general solution of (B.10) subject to (B.11) is

$$\bar{s}_U = \rho_1 e^{\eta z} + \rho_2 e^{-\eta z} \quad (\text{B.14})$$

291 where ρ_1 and ρ_2 are coefficients to be determined from boundary conditions.292 Considering that $\partial \bar{s}_H / \partial z = 0$ at $z = 0$ and $z = b$ by virtue of (A.5) and that

$$\left. \frac{\partial \bar{\sigma}}{\partial z} \right|_{z=b} = q(\bar{s}_C + \bar{s}_U)_{z=b} \quad (\text{B.15})$$

293 which, together with q , are derived in (D15) of Mishra and Neuman [9] and

$$\left. \frac{\partial \bar{s}_U}{\partial z} \right|_{z=0} = q_1(\bar{s}_C + \bar{s}_U)_{z=0} \quad (\text{B.16})$$

294 which, together with q_1 , are derived in (C.7) we obtain from (B.11)–(B.13)

$$\rho_1 = \frac{q_1(\eta + q)e^{-\eta b} \bar{s}_C(z=0) - q(\eta + q_1) \bar{s}(z=b)}{\Delta} \quad (\text{B.17})$$

295

$$\rho_2 = \frac{q_1(\eta - q)e^{-\eta b} \bar{s}_C(z=0) - q(\eta - q_1) \bar{s}(z=b)}{\Delta} \quad (\text{B.18})$$

296 where $\Delta = (\eta - q_1)(\eta + q)e^{-\eta b} - (\eta - q)(\eta + q_1)e^{\eta b}$.

297 The inverse Hankel transform of (B.14) is

$$\bar{s}_U = \int_0^\infty (\rho_1 e^{\eta z} + \rho_2 e^{-\eta z}) a J_0(ar) da. \quad (\text{B.19})$$

298 Defining a new variable $y = ar/K_D^{1/2} r_D$ transforms (B.19) into the result presented in (21).

299 It is noted that when $q_1 = 0$ the aquitard is replaced by an impermeable boundary, and

300 $\rho_1 = \rho_2 = \frac{2\bar{s}_C(z=b)}{\cosh(\eta b) - \frac{\eta}{q} \sinh(\eta b)}$. These simplifications reduce (B.19) to equation (3) of Mishra

301 and Neuman [9].

302 Appendix C. Aquitard Solution

303 Laplace–Hankel transform of governing flow equations for aquitard are

$$-a^2 \bar{s}_1 + K_{D1} \frac{\partial^2 \bar{s}_1}{\partial z^2} = p \frac{S_{s1}}{K_{r1}} \bar{s}_1 \quad 0 \leq z < -b_1 \quad (\text{C.1})$$

304 By virtue of no flow boundary at the bottom of the system, $\frac{\partial \bar{s}_1}{\partial z} \Big|_{z=-b_1} = 0$, the general

305 solution to (C.1) is

$$\bar{s}_1 = \rho_1 \cosh[\eta_1(z + b_1)] \quad (\text{C.2})$$

306 where $\eta_1^2 = \frac{a^2}{K_{D1}} + \frac{pS_{s1}}{K_{r1}K_{D1}}$. The boundary condition

$$\bar{s}_1(z=0) = \bar{s}(z=0) = (\bar{s}_C + \bar{s}_U)_{z=0} \quad (\text{C.3})$$

307 gives

$$s_1 = \frac{(\bar{s}_C + \bar{s}_U)_{z=0}}{\cosh(\eta b_1)} \cosh[\eta_1(z + b_1)]. \quad (\text{C.4})$$

308 Using (B.13) transforms (C.4) into the solution presented in (22).

309 The derivative of (C.4) is

$$\frac{d\bar{s}_1}{dz} = \eta_1 \tanh(\eta_1 b_1) (\bar{s}_C + \bar{s}_U) \quad z=0. \quad (\text{C.5})$$

310 The flux boundary condition at the aquifer-aquitard interface

$$\frac{\partial \bar{s}_1}{\partial z} \Big|_{z=0} = \frac{K_z}{K_{z1}} \frac{\partial \bar{s}}{\partial z} \Big|_{z=0} \quad (\text{C.6})$$

311 Combined with (B.9) gives

$$\frac{\partial \bar{s}}{\partial z} \Big|_{z=0} = q_1 (\bar{s}_C + \bar{s}_U)_{z=0} \quad (\text{C.7})$$

312 where $q_1 = \frac{K_{z1}}{K_z} \eta_1 \tanh(\eta_1 b_1)$.

313 **Appendix D. Lapalce Transformed Unsaturated Zone Drawdown**

314 Lapalce transformed drawdown $\bar{\sigma}$ in the unsaturated zone are given by Mishra and
 315 Neuman [9] as

$$\bar{\sigma}(r_D, z_D, p_D) = \begin{cases} \int_0^\infty e^{a_{kD}(z_D-1)/2} \frac{J_n[i\phi(z_D-1)] + \chi Y_n[i\phi(z_D-1)]}{J_n[i\phi(0)] + \chi Y_n[i\phi(0)]} \\ \quad \times (\bar{s}_C + \bar{s}_U)_{z_D=1} \frac{r_D^2 K_D}{r^2} dy & \text{for } a_{cD} \neq a_{kD} \\ \int_0^\infty \frac{e^{\delta_{1D}(z_D-1) + \chi e^{\delta_{2D}(z_D-1)}}}{1 + \chi} \\ \quad \times (\bar{s}_C + \bar{s}_U)_{z_D=1} \frac{r_D^2 K_D}{r^2} dy & \text{for } a_{cD} = a_{kD} = \kappa_D \end{cases} \quad (\text{D.1})$$

316 where $r_D = r/b$, $z_D = z/b$, $\mu^2 = y^2 + \frac{pD}{t_s K_D r_D^2}$, $t_s = \alpha_s t / r^2$, $\alpha_s = K_r / S_s$, $q_D = qb$,
 317 $a_{kD} = a_k b$, $a_{cD} = a_c b$, $\phi(z_D) = \sqrt{\frac{4B_D}{\lambda_D^2}} e^{\lambda_D z_D / 2}$, $\lambda_D = a_{kD} - a_{cD}$, $B_D = pD \frac{S_D a_{cD} e^{a_{kD}(\psi_{kD} - \psi_{aD})}}{t_s K_D r_D^2}$,
 318 $S_D = S_y / S$, $\psi_{kD} = \psi_k / b$, $\psi_{aD} = \psi_a / b$, $\delta_{1D, 2D} = \delta_{1, 2} b = \frac{\kappa_D \mp \sqrt{\kappa_D^2 + 4(B_D + y^2)}}{2}$, $\nu = \sqrt{\frac{a_{kD}^2 + 4y^2}{\lambda_D^2}}$,
 319 and $p_D = pt$ are dimensionless quantities, p being the Laplace transform parameter;

$$\begin{aligned} \bar{s}_C(z = b) = C_0 \frac{r^2}{K_D r_D^2} & \left\{ \frac{y_D r_{wD}}{y^2} J_1(y_D r_{wD}) K_0(r_{wD} \phi_0) + \Gamma(0) \right\} \\ & + \sum_{n=1}^{\infty} C_n \frac{r^2}{K_D r_D^2} \left\{ \frac{y_D r_{wD}}{y^2} J_1(y_D r_{wD}) K_0(r_{wD} \phi_0) + \Gamma(n) \right\} \end{aligned} \quad (\text{D.2})$$

320 where $\Gamma(n) = \frac{r_{wD} \phi_n J_0(y_D) K_1(\phi_n) - y_D r_{wD} J_1(y_D) K_0(\phi_n)}{\mu^2 + n^2 \pi^2}$, $y_D = y K_D^{1/2} r_D$, J_0 and J_1 being Bessel
 321 functions of first kind and, respectively, orders zero and one; and

$$\chi = \begin{cases} -\frac{(a_{kD} + n\lambda_D) J_n[i\phi(L_D)] - 2i\sqrt{B_D e^{\lambda_D L_D}} J_{n+1}[i\phi(L_D)]}{(a_{kD} + n\lambda_D) Y_n[i\phi(L_D)] - 2i\sqrt{B_D e^{\lambda_D L_D}} Y_{n+1}[i\phi(L_D)]} & a_{kD} \neq a_{cD} \\ i & a_{kD} \neq a_{cD}, L_D \rightarrow \infty \\ -\frac{\delta_{1D}}{\delta_{2D}} e^{(\delta_{1D} - \delta_{2D}) L_D} & a_{kD} = a_{cD} \\ 0 & a_{kD} = a_{cD}, L_D \rightarrow \infty \end{cases} \quad (\text{D.3})$$

$$q_D = \begin{cases} \left(\frac{a_{kD}}{2} + \frac{n\lambda_D}{2} \right) - i\sqrt{B_D} \frac{J_{n+1}[i\phi(0)] + \chi Y_{n+1}[i\phi(0)]}{J_n[i\phi(0)] + \chi Y_n[i\phi(0)]} & a_{kD} \neq a_{cD} \\ \frac{\delta_{1D} + \chi \delta_{2D}}{1 + \chi} & a_{kD} = a_{cD} = \kappa_D \end{cases} \quad (\text{D.4})$$

322 where $L_D = L/b$, J_n and Y_n being first and second kind Bessel functions of order n .

323 **References**

- 324 [1] G. Nwankwor, J. Cherry, R. Gillham, A comparative study of specific yield determina-
325 tions for a shallow sand aquifer, *Ground Water* 22 (6) (1984) 764–772.
- 326 [2] F. Akindunni, R. Gillham, Unsaturated and saturated flow in response to pumping of an
327 unconfined aquifer: Numerical investigation of delayed drainage, *Ground Water* 30 (6)
328 (1992) 873–884.
- 329 [3] G. Tartakovsky, S. Neuman, Three-dimensional saturated-unsaturated flow with axial
330 symmetry to a partially penetrating well in a compressible unconfined aquifer, *Water*
331 *resources research* 43 (1) (2007) W01410.
- 332 [4] S. Mathias, A. Butler, Linearized Richards’ equation approach to pumping test analysis
333 in compressible aquifers, *Water Resources Research* 42 (6) (2006) W06408.
- 334 [5] P. Mishra, S. Neuman, Improved forward and inverse analyses of saturated-unsaturated
335 flow toward a well in a compressible unconfined aquifer, *Water Resources Research*
336 46 (7) (2010) W07508, ISSN 0043-1397.
- 337 [6] U. Kroszynski, G. Dagan, Well pumping in unconfined aquifers: The influence of the
338 unsaturated zone, *Water Resources Research* 11 (3) (1975) 479–490.
- 339 [7] I. Papadopoulos, H. Cooper Jr, Drawdown in a well of large diameter, *Water Resources*
340 *Research* 3 (1) (1967) 241–244.
- 341 [8] T. Narasimhan, M. Zhu, Transient flow of water to a well in an unconfined aquifer:
342 applicability of some conceptual models, *Water Resources Research* 29 (1) (1993) 179–
343 191.
- 344 [9] P. Mishra, S. Neuman, Saturated-unsaturated flow toward a well with storage in a
345 compressible unconfined aquifer, *Water Resources Research* 86 (7) (2011) W12508, ISSN
346 0043-1397.

- 347 [10] W. Gardner, Some steady-state solutions of the unsaturated moisture flow equation
348 with application to evaporation from a water table, *Soil Science* 85 (4) (1958) 228.
- 349 [11] D. Russo, Determining soil hydraulic properties by parameter estimation: On the se-
350 lection of a model for the hydraulic properties, *Water Resources Research* 24 (3) (1988)
351 453–459.
- 352 [12] R. Brooks, A. Corey, Hydraulic properties of porous media, *Hydrology Papers* 30, Col-
353 orado State University, Fort Collins (March).
- 354 [13] M. van Genuchten, A closed-form equation for predicting the hydraulic conductivity of
355 unsaturated soils, *Soil Sci. Soc. Am. J* 44 (5) (1980) 892–898.
- 356 [14] M. Hantush, Non-steady radial flow in an infinite leaky aquifer., *Transactions, American*
357 *Geophysical Union* 36 (1) (1955) 95–100.
- 358 [15] M. Hantush, Modification of the theory of leaky aquifers, *Journal of Geophysical Re-*
359 *search* 65 (11) (1960) 3713–3725.
- 360 [16] S. Neuman, P. Witherspoon, Applicability of current theories of flow in leaky aquifers,
361 *Water Resources Research* 5 (4) (1969) 817–829.
- 362 [17] S. Neuman, P. Witherspoon, Theory of flow in a confined two aquifer system, *Water*
363 *Resources Research* 5 (4) (1969) 803–816.
- 364 [18] I. Yatov, On drawdown around wells in leaky water table aquifer, *Comptes rendu de*
365 *Academie Bulgara des Sciences* 21 (8) (1968) 765–768.
- 366 [19] N. Boulton, The drawdown of the water-table under non-steady conditions near a
367 pumped well in an unconfined formation., in: *ICE Proceedings: Engineering Divisions*,
368 vol. 3, Ice Virtual Library, 564–579, 1954.
- 369 [20] C. Ehlig, J. Halepaska, A numerical study of confined-unconfined aquifers including
370 effects of delayed yield and leakage, *Water Resources Research* 12 (6) (1976) 1175–1183,
371 ISSN 0043-1397.

- 372 [21] V. Zlotnik, H. Zhan, Aquitard effect on drawdown in water table aquifers, Water Re-
373 sources Research 41 (6) (2005) W06022, ISSN 0043-1397.
- 374 [22] H. Zhan, A. Bian, A method of calculating pumping induced leakage, Journal of Hy-
375 drology 328 (3-4) (2006) 659–667.
- 376 [23] J. Butler Jr, M. Tsou, Pumping-induced leakage in a bounded aquifer: An example of
377 a scale-invariant phenomenon, Water resources research 39 (12) (2003) 1344.
- 378 [24] B. Malama, K. Kuhlman, W. Barrash, Semi-analytical solution for flow in leaky un-
379 confined aquifer-aquitard systems, Journal of Hydrology 346 (1-2) (2007) 59–68, ISSN
380 0022-1694.
- 381 [25] H. Zhan, V. Zlotnik, Groundwater flow to a horizontal or slanted well in an unconfined
382 aquifer, Water Resour. Res 38 (7) (2002) 1108.
- 383 [26] F. de Hoog, J. Knight, A. Stokes, An improved method for numerical inversion of
384 Laplace transforms, SIAM Journal on Scientific and Statistical Computing 3 (1982)
385 357.
- 386 [27] S. Neuman, Theory of flow in unconfined aquifers considering delayed response of the
387 water table, Water Resources Research 8 (4) (1972) 1031–1045, ISSN 0043-1397.
- 388 [28] B. Malama, K. Kuhlman, W. Barrash, Semi-analytical solution for flow in a leaky
389 unconfined aquifer toward a partially penetrating pumping well, Journal of Hydrology
390 356 (1-2) (2008) 234–244.